AIAA Guidance, Navigation, and Control Conference and Exhibit
6-9 August 2001 Montreal, Canada

A01-37045

AIAA-2001-4095

FIXED-GAIN/ADAPTIVE CONTROL FOR SIMULTANEOUS REJECTION OF BROADBAND AND SINUSOIDAL DISTURBANCES

Ravinder Venugopal*and Dennis S. Bernstein‡

ABSTRACT

In this paper we experimentally investigate the feasibility of using a hybrid fixed-gain/adaptive control architecture for simultaneous rejection of broadband and sinusoidal disturbances. The motivation for this study comes from active noise control (ANC) applications in which the disturbance has both broadband and sinusoidal components, for example, wind noise and engine noise in an aircraft cabin. The advantage of this approach is that it improves performance while reducing real-time computational load. The experiment is carried out on a three dimensional acoustic space contained in a steel drum, on which speakers and microphones are mounted as actuators and sensors respectively. A fixed-gain H_2 optimal (LQG) controller is used to attenuate the broadband component of the noise while a low-order extended ARMARKOV adaptive controller (EAAC) is used to attenuate a tonal disturbance of unknown frequency.

INTRODUCTION

The rejection of disturbances is a fundamental objective of control system design, and there are several well known methods for achieving disturbance rejection using fixed-gain and adaptive approaches. Fixed-gain controllers are designed to attenuate or cancel disturbances whose spectrum is known and does not change. These methods include internal model based controllers for sinusoidal disturbances, and H_2 optimal (LQG) controllers for broadband disturbances; see [1, 2, 3, 4, 5, 6, 7] for example. Internal model controllers require exact knowledge of the frequencies of the tones in a sinusoidal disturbance, but in many applications this information is not known and may be time varying. LQG controllers are effective for broadband disturbances but do not perform well with tonal disturbances, especially if their frequencies are not known. On the other hand, several adaptive controllers [4, 8, 9, 10, 11, 12, 13], perform well on both broadband and tonal disturbances and can adapt to changes in the spectrum of the disturbance. However, adaptive controllers are computationally very intensive, especially when used to attenuate broadband disturbances which require a large number of controller parameters. Fixed-gain controllers are much less computationally intensive and even high-order MIMO systems can be implemented at high sampling rates using commercially available real-time systems.

Active noise control (ANC) is an area of application of disturbance rejection algorithms that has been studied extensively in recent years [4]-[16]. In several ANC applications, the disturbance signal is comprised of both broadband and tonal components, for example, wind noise and engine noise in an aircraft, or flow noise and motor noise in an air-conditioning system. While a single high-order adaptive controller may be used in these cases, these controllers need to run at a sampling rate of at least 800 Hz, and thus have severe computational requirements which may prohibit implementation. In this paper we propose an architecture that uses a fixed-gain LQG controller to attenuate the broadband disturbance and a low-order Extended ARMARKOV Adaptive Controller (EAAC) [13, 18] to cancel the tonal disturbance. The EAAC has been chosen based on the comparison in [11]. The computational requirements of both these controllers are less than that of a high-order adaptive controller, and since they operate independently, they can be implemented in a decentralized manner on different

*dSPACE Inc., 22260 Haggerty Rd., Suite 120, Northville, MI 48167, rvenugopal@dspaceinc.com, Member

†Aerospace Engg. Department, University of Michigan, Ann Arbor, MI 48109, dsbaero@umich.edu

processors.

The EAAC is based on the ARMARKOV adaptive control (AAC) algorithm developed in [12] and extended in [13]. The underlying model structure of AAC is the ARMARKOV model, which is a structurally constrained ARMA model with explicit impulse response (Markov) parameters. The results reported in [11, 12, 13, 14, 17] demonstrate the ability of the algorithm to suppress single-tone, dual-tone, and broadband disturbances without prior knowledge of the spectral characteristics of the disturbance. These results depend upon the availability of a model of only the secondary path transfer function from the control input to the error variables, represented by the Toeplitz matrix B_{zu}.

In [13] the AAC algorithm is extended by including simultaneous identification of the secondary path. To do this, the secondary path matrix B_{zu} is updated *at each time step* by means of the ARMARKOV/Toeplitz recursive identification method of [19]. Thus, the extended ARMARKOV adaptive control (EAAC) algorithm starts out with no prior knowledge of the plant dynamics *and* no measurement of the disturbance or knowledge of its spectrum, allowing us to implement the EAA controller around the closed-loop system consisting of the plant and the LQG controller. We close the inner-loop with the LQG controller, then switch on the EAAC to identify the required path, and finally adapt the EAAC parameters to attenuate the effects of the disturbance that are not attenuated by the LQG controller.

This paper presents the results of an experimental study of the hybrid LQG/EAAC control architecture on a three dimensional acoustic test bed. The test bed consists of a steel drum with speakers as actuators mounted on the top and bottom. Microphones which serve as sensors are inserted in to the drum through holes on the side. The LQG and EAA controllers were implemented on a dSPACE real-time multiprocessor system with four Alpha/C40 combination processors.

This study has the following specific objectives. First, to study the issues related to designing a robust H_2 optimal controller which achieves broadband disturbance rejection in a three-dimensional acoustic space. Second, to assess the feasibility of implementing a low-order closed-loop stable adaptive controller capable of attenuating tonal disturbances in the presence of broadband noise while working in conjunction with an LQG controller on a high-order plant.

In the next section, we review the standard problem framework [1] for analyzing the disturbance rejection problem. In Section 3, we provide a brief description of the experimental test-bed. Section 4 describes the design procedure for the robust LQG controller, while Sections 5 and 6 provide an overview of the EAAC algorithm. In Section 7 we describe the computational hardware architecture used to implement the hybrid controller, and then present our results in Section 8. We conclude in Section 9 with a discussion of implementation issues and future work.

DISTURBANCE REJECTION PROBLEM

Consider the linear discrete-time two vector-input, two vector-output (TITO) system shown in Figure 1. The *disturbance* $w(k)$, the *control* $u(k)$, the *measurement* $y(k)$ and the *performance* $z(k)$ are in $\mathcal{R}^{m_w}$, $\mathcal{R}^{m_u}$, $\mathcal{R}^{l_y}$ and $\mathcal{R}^{l_z}$, respectively. The system can be written in state space form as

$$x(k+1) = Ax(k) + Bu(k) + D_1 w(k), \quad (1)$$
$$z(k) = E_1 x(k) + E_2 u(k) + E_0 w(k), \quad (2)$$
$$y(k) = Cx(k) + Du(k) + D_2 w(k), \quad (3)$$

or equivalently in terms of transfer matrices

$$z = G_{zw} w + G_{zu} u, \quad (4)$$
$$y = G_{yw} w + G_{yu} u. \quad (5)$$

The controller G_c generates the control signal $u(k)$ based on the measurement $y(k)$, that is,

$$u = G_c y. \quad (6)$$

The objective of the standard problem is to determine a controller G_c that produces a control signal $u(k)$ based on the measurement $y(k)$ such that a performance measure involving $z(k)$ is minimized.

EXPERIMENTAL TEST-BED

The hybrid LQG/EAAC control system is tested on a three dimensional acoustic chamber enclosed a steel drum. The drum is 30 inches tall and has a diameter of 20 inches. Four Kicker Freeair 6.5c speakers are mounted on the top and bottom of the drum as shown in Figure 2. The centers of speakers are located 7 inches from the center of the top of the drum along a radial line. The line joining the centers of the speakers on the top makes a right angle to the

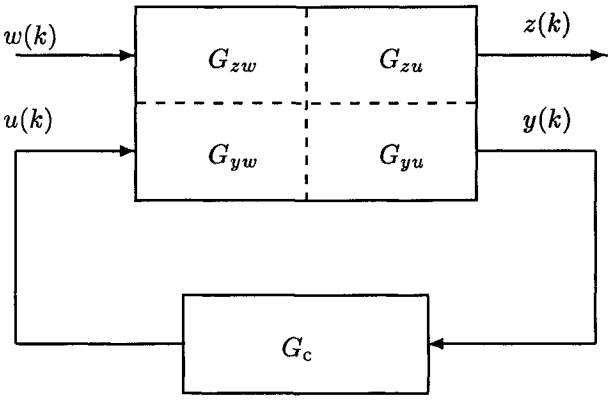

Figure 1: Standard problem with fixed-gain controller

line joining the centers of the speakers on the bottom. Six Optimus 33-013 tie-clip microphones are inserted in to the drum through six holes on the side of the drum. Two holes are at a height of 6 inches, two at a height of 15 inches and two at a height of 24 inches. One hole of each of these pairs is at an angle of 45° to the line joining the centers of the speakers at the top, while the other is at an angle of -45° to this line. This sensor-actuator placement is designed to allow several MIMO and SISO test configurations. However, for the experiment described here, two actuators and two sensors are arbitrarily chosen. One speaker on the top is used as a disturbance actuator (driven by the signal $w(k)$) while one on the bottom is used as a control actuator (driven by the signal $u(k)$). One microphone located near the top of the drum is used as a measurement microphone ($y(k)$) while one near the bottom is used as a performance microphone ($z(k)$). The sensor signals are amplified through a TASCAM MA-8 microphone pre-amplifier, and filtered through two channels of a four channel Krohn-Hite Model 3364 four-pole low pass Butterworth anti-aliasing filter with a cut-off frequency of 250 Hz before being fed to a dSPACE DS2003 16-bit A/D board in a dSPACE Multiprocessor real-time system. The disturbance and control signals are fed from a DS2103 D/A board to the two other channels of the Krohn-Hite filter, and then amplified through a Crossfire CFA404 four channel car-audio power amplifier to drive the actuators.

FIXED-GAIN CONTROLLER SYNTHESIS

In this section we outline the design procedure used to synthesize a robust fixed-gain LQG controller for broadband disturbance attenuation. The

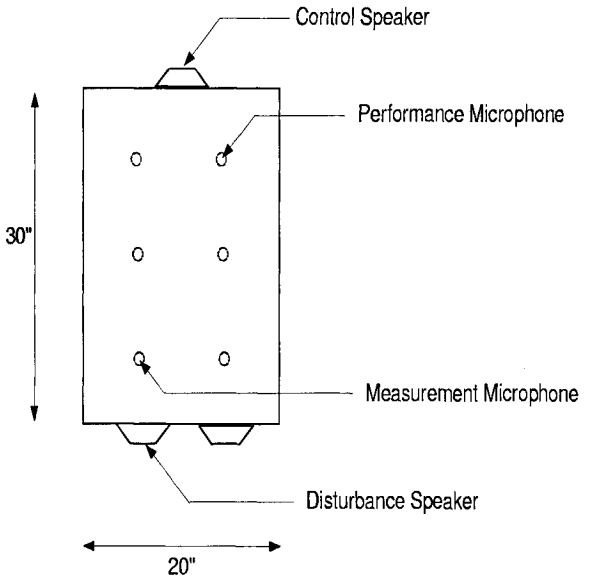

Figure 2: Front view of acoustic test-bed

design objective is to obtain a controller that minimizes the H_2 norm of the closed-loop transfer function $\tilde{G}_{zw}$ and provides robust stability with respect to modeling errors.

The first step in the procedure is the identification of the matrices A, B, C, D, D_1, D_2, E_1 and E_2 of the system (1)-(3). The matrix E_0 was taken to be 0. The N4SID subspace system identification method [20] was used to identify the MIMO system by driving the actuators simultaneously with uncorrelated uniform random noise between -1V and 1V, and measuring the sensor signals at a sampling frequency of 800 Hz using the dSPACE system. The MATLAB System Identification Toolbox was used to implement the N4SID algorithm and a 40^{th} model was identified. Figures 3-6 show the measured and identified frequency responses.

Figures 7 and 8 show the pole-zero maps of the transfer functions G_{yw} and G_{zu}, and we note that both these transfer functions are non-minimum phase. These paths are critical in determining the achievable performance of an LQG controller [16], and if either one or both is non-minimum phase, closed-loop spillover is unavoidable. Thus, the control weighting in the LQG design process must be chosen carefully to minimize spillover, especially in the frequency band of the tonal disturbance.

The full-order LQG controller is designed by solving the estimator and regulator discrete time al-

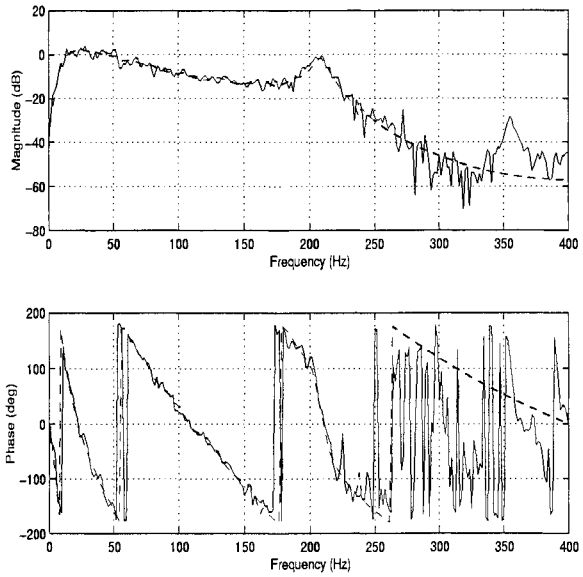

Figure 3: Frequency response of G_{zw}. Solid-line: measured, dashed-line: identified

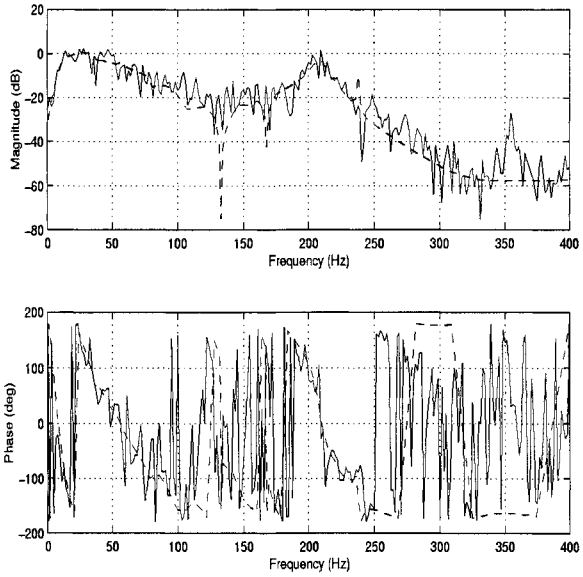

Figure 5: Frequency response of G_{zu}. Solid-line: measured, dashed-line: identified

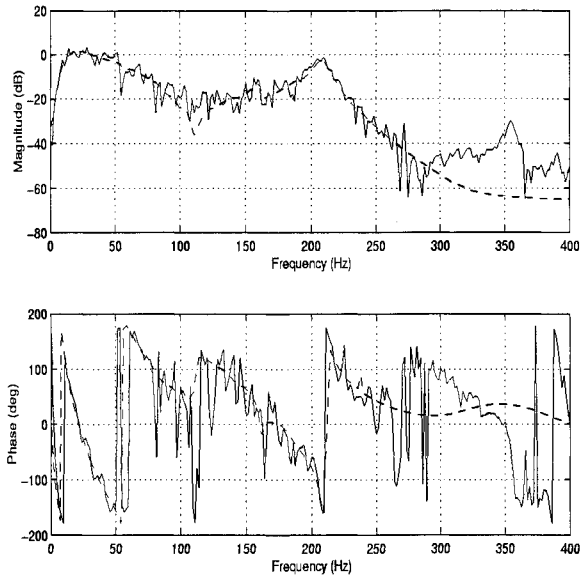

Figure 4: Frequency response of G_{yw}. Solid-line: measured, dashed-line: identified

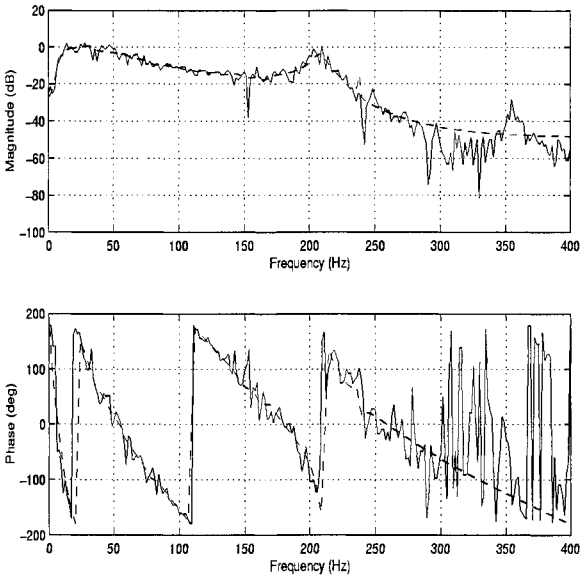

Figure 6: Frequency response of G_{yu}. Solid-line: measured, dashed-line: identified

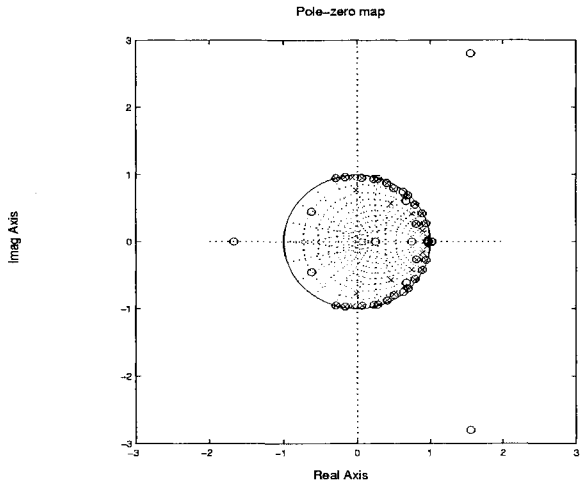

Figure 7: Pole-zero map of G_{yw}.

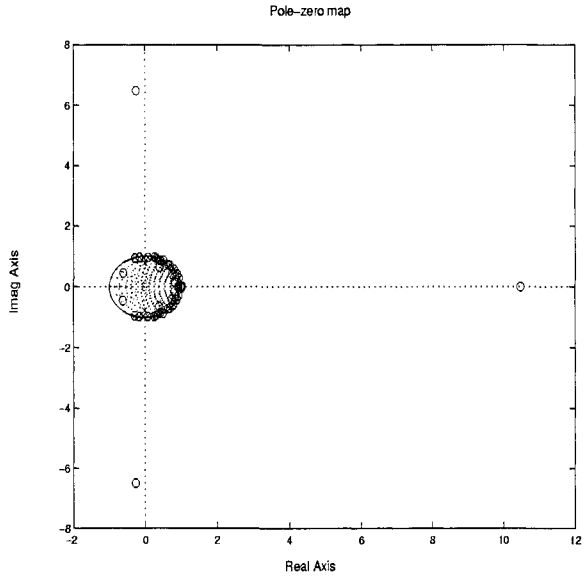

Figure 8: Pole-zero map of G_{zu}.

gebraic Riccati equations in MATLAB. The control weighting matrix E_2 is chosen to achieve maximum performance while ensuring stability robustness to the modeling error between the identified model and the actual system.

The following H_∞ based technique [6, 7] is used to choose E_2. Noting that closed-loop stability depends on G_{yu}, the modeling error $\Delta(e^{j\omega})$ is defined as

$$\Delta(e^{j\omega}) \triangleq G_{yu}(e^{j\omega}) - \bar{G}_{yu}(e^{j\omega}), \tag{7}$$

where $G_{yu}(e^{j\omega})$ is the measured frequency response and $\bar{G}_{yu}(e^{j\omega})$ is the identified frequency response. Next, a filter $W(z)$ is designed such that

$$|W(e^{j\omega})| > |\Delta(e^{j\omega})|, \tag{8}$$

for $0 \leq \omega \leq 2\pi$. The closed-loop system with uncertainty can be represented as shown in Figure 9 with $\bar{\Delta}(z) \triangleq W^{-1}(z)\Delta(z)$. Thus, the modeling error is introduced as a feedback uncertainty and by (8) it follows that $\|\bar{\Delta}\|_\infty < 1$, where $\|\cdot\|_\infty$ represents the H_∞ norm of a system. Using the Small-Gain Theorem, we note that if

$$\|\tilde{\mathcal{G}}\|_\infty < 1, \tag{9}$$

where $\tilde{\mathcal{G}}(z) \triangleq G_c(z)(I - \bar{G}_{yu}(z)G_c(z))^{-1}W(z)$, the closed-loop system will be stable. Hence, the value of E_2 is increased from zero until (9) is satisfied to obtain a robust controller with sufficient performance. Closed-loop performance is very sensitive to the choice of $W(z)$, and thus, to achieve the best possible performance, $W(z)$ should be chosen non-conservatively.

The closed-loop performance using the robust LQG controller is shown in Figure 10 by plotting the frequency response of G_{zw}. The simulated and experimental results match each other closely, and the limited performance obtained is due to the non-minimum phase nature of G_{yw} and G_{zu}. The controller is found to be unstable, and thus cannot be balanced for better numerical conditioning. It also cannot be turned off during operation without resetting the internal states of the controller. Stable controllers are obtained by using larger values of E_2, but these controllers yield poor performance.

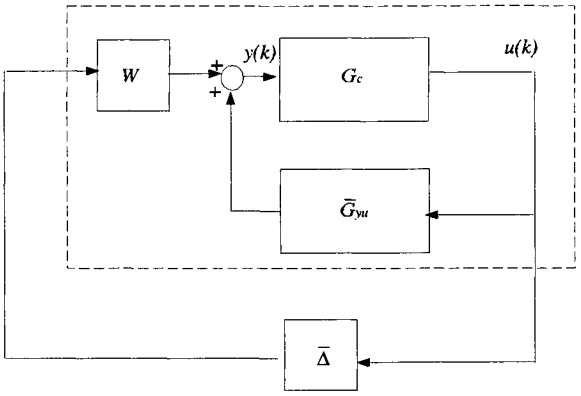

Figure 9: Closed-loop system with uncertainty

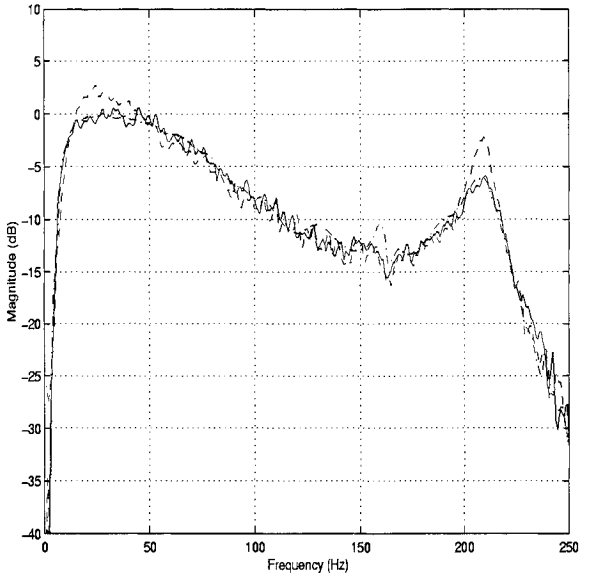

Figure 10: Closed-loop performance of robust LQG controller. Dashed line: open-loop, dash-dot line: closed-loop (simulation), solid line: closed-loop (experimental)

ADAPTIVE ARMARKOV ALGORTIHM

In this section we review the ARMARKOV adaptive disturbance rejection feedback algorithm [12] for the TITO system (1)-(3) represented in ARMARKOV form as

$$Z(k) = W_{zw}\Phi_{zw}(k) + B_{zu}U(k), \quad (10)$$
$$Y(k) = W_{yw}\Phi_{yw}(k) + B_{yu}U(k). \quad (11)$$

We use a strictly proper controller in ARMARKOV form of order n_c with μ_c Markov parameters, so that the control $u(k)$ is given by

$$u(k) = \sum_{j=1}^{n_c} -\alpha_{c,j}(k)u(k-\mu_c-j+1) + \sum_{j=1}^{\mu_c-1} H_{c,j-1}(k)y(k-j+1) + \sum_{j=1}^{n_c} \mathcal{B}_{c,j}(k)y(k-\mu_c-j+1), \quad (12)$$

where $H_{c,j} \in \mathcal{R}^{m_u \times l_y}$ are the Markov parameters of the controller. Next, define the *controller parameter block vector*

$$\theta(k) \triangleq [-\alpha_{c,1}(k)I_{m_u} \quad \cdots \quad -\alpha_{c,n_c}(k)I_{m_u} \quad H_{c,0}(k) \quad \cdots \quad H_{c,\mu_c-2}(k) \quad \mathcal{B}_{c,1}(k) \quad \cdots \quad \mathcal{B}_{c,n_c}(k)].$$

As shown in [12], it follows that $U(k)$ is given by

$$U(k) = \sum_{i=1}^{p_c} L_i\theta(k-i+1)R_i\Phi_{uy}(k), \quad (13)$$

and the control input to the system $u(k)$ at the instant k is given by

$$u(k) = \theta(k)R_1\Phi_{uy}(k), \quad (14)$$

with

$$\Phi_{uy}(k) \triangleq [u(k-\mu_c) \quad \cdots \quad u(k-\mu_c-n_c-p_c+2) \quad y(k-1) \quad \cdots \quad y(k-\mu_c-n_c-p_c+2)]^T,$$

and where L_i and R_i are constraint matrices that maintain the block-Toeplitz structure of the control weight matrix in (13) [12]. Thus, from (10) and (13) we obtain

$$Z(k) = W_{zw}\Phi_{zw}(k) + B_{zu}\sum_{i=1}^{p_c} L_i\theta(k-i+1)R_i\Phi_{uy}(k). \quad (15)$$

Next, we define a cost function that evaluates the performance of the current value of $\theta(k)$ based upon the behavior of the system during the previous p_c steps. Therefore, we define the *estimated performance* $\hat{Z}(k)$ by

$$\hat{Z}(k) \triangleq W_{zw}\Phi_{zw}(k) + B_{zu}\sum_{i=1}^{p_c} L_i\theta(k)R_i\Phi_{uy}(k), \quad (16)$$

which has the same form as (15) but with $\theta(k-i+1)$ replaced by the current parameter block vector $\theta(k)$. Using (16) we define the *estimated performance cost function*

$$J(k) = \frac{1}{2}\hat{Z}^{\mathrm{T}}(k)\hat{Z}(k). \quad (17)$$

The gradient of $J(k)$ with respect to $\theta(k)$ is given by

$$\frac{\partial J(k)}{\partial \theta(k)} = \sum_{i=1}^{p_c} L_i^{\mathrm{T}} B_{zu}^{\mathrm{T}} \hat{Z}(k)\Phi_{uy}^{\mathrm{T}}(k)R_i^{\mathrm{T}}. \quad (18)$$

Note that $\hat{Z}(k)$ cannot be evaluated using (16) since $w(k)$ is not available which implies that $\Phi_{zw}(k)$ is unknown. However, it follows from (10) and (16) that

$$\hat{Z}(k) = Z(k) - B_{zu}\left(U(k) - \sum_{i=1}^{p_c} L_i\theta(k)R_i\Phi_{uy}(k)\right),$$

which can be used to evaluate (18).

The gradient (18) is used in the update law

$$\theta(k+1) = \theta(k) - \eta(k)\frac{\partial J(k)}{\partial \theta(k)}, \quad (19)$$

where $\eta(k)$ is the *adaptive step size* given by

$$\eta(k) = \frac{1}{p_c\|B_{zu}\|_{\mathrm{F}}^2\|\Phi_{uy}(k)\|_2^2}. \quad (20)$$

It is shown in [12] that the update law (19) with the step size (20) brings $\theta(k)$ closer to the minimizer of $J(k)$ with each time step. Note that for implementing the algorithm in practice (18, 19, 20), we only need to know the secondary feedback matrix B_{zu} apart from the measurements z and y.

EXTENDED AAC ALGORITHM

In this section we discuss the self-tuning ARMARKOV/Toeplitz controller along with simultaneous identification. The secondary path matrix B_{zu} can be obtained on-line using the time domain identification technique discussed in [19]. In order to identify B_{zu} in the presence of the disturbance $w(k)$, an uncorrelated signal u_{ID} is added to the control signal. The signal u_{ID} is small enough not to deteriorate the performance beyond acceptable limits. An estimate $\widehat{W}_{zu}(k)$ can be obtained at every time instant k using the identification method of [19] with $u(k)$ replaced by $u_{\mathrm{ID}}(k)$. An estimate of B_{zu}, namely $\widehat{B}_{zu}(k)$ can thus be extracted from $\widehat{W}_{zu}(k)$ and passed on to the AAC algorithm for $\theta(k)$ gradient update. Hence for practical implementation, B_{zu} in equations (18 - 20) is replaced by the current estimate $\widehat{B}_{zu}(k)$.

HYBRID CONTROLLER IMPLEMENTATION

The hardware architecture for the implementation of the hybrid LQG/EAA controller is shown in Figure 11. The system is implemented on a dSPACE Multiprocessor system with four DS1003/DS1004 Alpha Combos. The DS1004 Alpha processor boards perform all computations while the DS1003 TMS320C40 processor boards perform data transfer and inter-processor communication and synchronization. One DS1004 is used to implement the LQG controller, the second is used to implement the AAC controller, the third is used for real-time identification of the matrix B_{zu} which is used by the AAC controller, and the fourth is used to generate the disturbance signal. The DS2003 A/D board reads the filtered sensor signals, $y(k)$ and $z(k)$, while the DS2103 D/A board generates the actuator signals, $w(k)$ and $u(k)$. The control algorithm is modeled in Simulink and implemented using dSPACE's RTI-MP (Real-Time Interface for Multi-Processor systems). The AAC algorithm and EAAC system identification algorithm are written as Simulink S-functions in C.

The LQG controller is a 40^{th} order controller, and taking the plant to be 40^{th} order, the closed-loop system with the LQG controller is of order 80. However, we use a low-order AAC controller with $n_c = 12$ and $\mu_c = 22$. The parameters used to characterize B_{zu} are $n = 20$, $\mu = 55$ and $p = 4$. We add uniform random noise between ± 1V to a single tone of amplitude 0.15V at 80Hz to obtain the disturbance signal. The tone is representative of engine noise generated at 4800 RPM. The multiprocessor system is run at a sampling rate of 800 Hz.

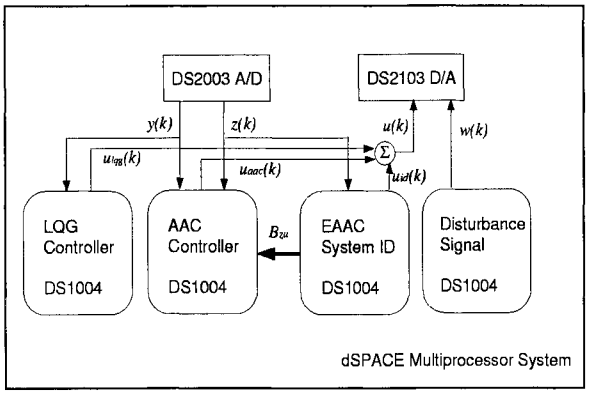

Figure 11: Hardware architecture for hybrid controller implementation.

RESULTS

We assessed the performance of the EAAC controller, the LQG controller and the hybrid controller using three separate tests. A disturbance signal comprising of broadband noise and a single tone at 80 Hz was used for all three tests. For the first test, the disturbance signal was turned on, and then EAAC identification was performed for 5 seconds in the presence of the disturbance. The EAAC was then turned on, and the performance of the low-order EAAC after 30 seconds of adaptation is shown in Figure 12 as a power spectral density (PSD) plot of $z(k)$. We see that the EAAC is able to reduce the tone to approximately the level of the broadband disturbance, but then attempts to reduce the broadband component also and is thus neither able to effectively cancel the tone nor significantly attenuate the broadband noise.

In Figure 13 we see that the broadband performance of the LQG controller is similar to the performance shown in Figure 10, but the controller has little effect on the tonal disturbance.

To test the hybrid controller, the LQG controller was turned on with the disturbance on, and after a few seconds, EAA identification of B_{zu} was performed. The EAA controller was then turned on, and was allowed to adapt for 30 seconds before freezing the controller parameters. Figure 14 shows the performance of the hybrid controller, and we can see that there is greater attenuation of both broadband and tonal components than that of either the EAA or LQG controller on any one of the components.

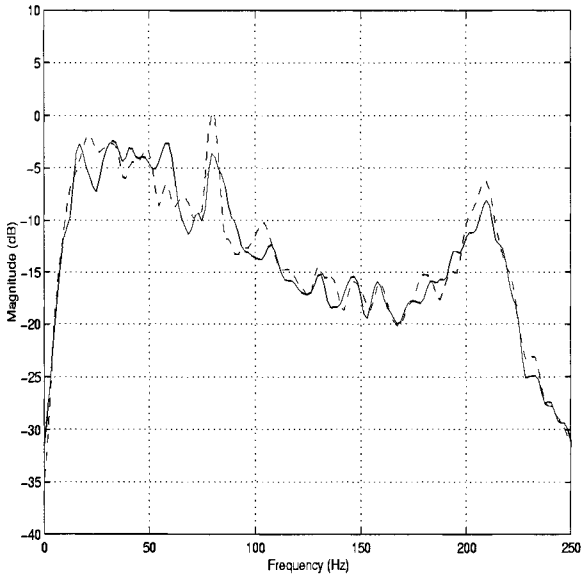

Figure 12: Open-loop and closed-loop performance with EAA controller.

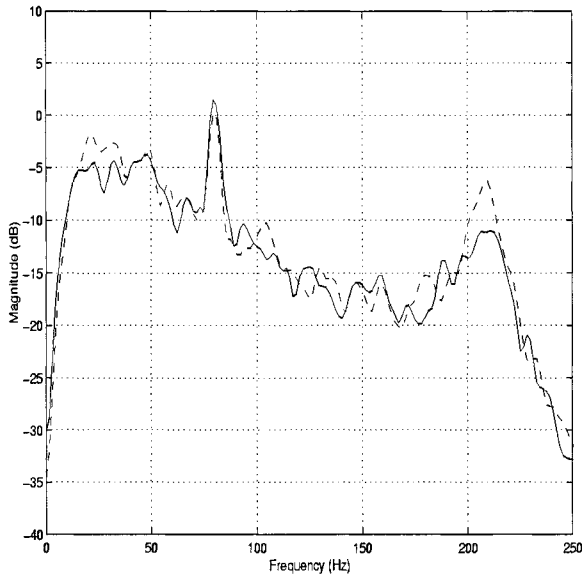

Figure 13: Open-loop and closed-loop performance with LQG controller.

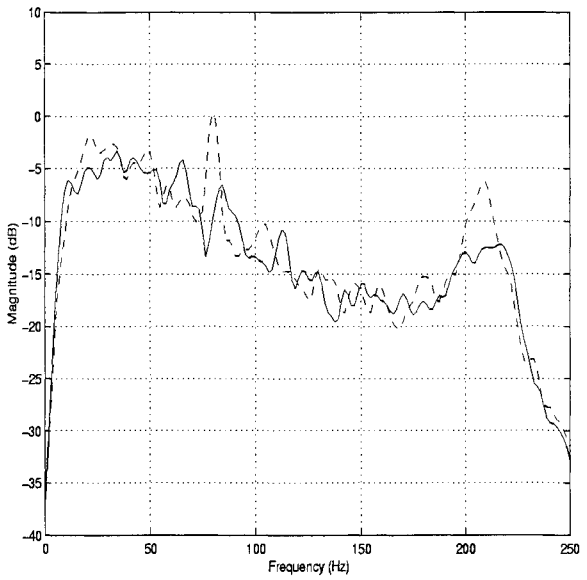

Figure 14: Open-loop and closed-loop performance hybrid LQG/EAA controller.

CONCLUSIONS

In this paper, we have experimentally evaluated a hybrid fixed-gain/adaptive controller architecture for simultaneous rejection of broadband and sinusoidal disturbances on a three dimensional acoustic space. The hybrid controller shows improved performance over its component LQG and EAA controllers. In the course of the design and implementation, we made the following observations

1. Three dimensional acoustic systems have high order dynamics. The identified state space model that is used to represent the acoustic system used in this experiment in the frequency range of 0-400 Hz is a 40^{th} order model.

2. Sensor and actuator placement should be chosen using acoustic and control performance requirements. Acoustic requirements define performance sensor and control speaker locations for global noise reduction, while control considerations require G_{yw} and G_{zu} to be minimum phase to prevent spillover [16].

3. High control authority LQG controllers may result in unstable closed-loops during implementation due to modeling errors. Robust control design techniques can be used to account for these errors and ensure stability.

4. The weighting filter $W(z)$ used in the design of the LQG controller has a significant effect on the closed-loop performance and should be chosen non-conservatively to ensure maximum performance.

We note that the processors used to implement the proposed control architecture are extremely powerful. However, implementation of a high order EAA controller that would yield the same performance as the hybrid controller would have been impossible, even on these processors. The results demonstrate the feasibility of this approach, and future work will involve using reduced order fixed-structure controller synthesis for the fixed-gain controller using the design methodology in [6, 7]. A reduced order fixed-gain controller will allow the use of EAA controllers with fewer parameters in the proposed hybrid architecture, and result in further reduction in computational requirements.

ACKNOWLEDGEMENTS

The first author would like to thank Dr. R. S. Erwin of the Air Force Research Laboratory for the informative discussions on robust LQG design, and Mr. Islam Hussein of the University of Michigan for assistance with laboratory hardware.

References

[1] B. Francis, *A Course in H_∞ Control Theory*, New York: Springer-Verlag, 1987.

[2] A. G. Sparks and D. S. Bernstein, "Optimal Rejection of Stochastic and Deterministic Disturbances," *Journ. Dyn., Meas. Contr.*, Vol. 119, pp. 140 - 143, 1997.

[3] R. L. Clark and D. S. Bernstein, "Hybrid control: Separation in design," *Journ. Sound and Vib.*, Vol. 214, pp. 784-791, 1998.

[4] R. L. Clark, W. R. Saunders, and G. P. Gibbs, *Adaptive Structures Dynamics and Control*, John Wiley and Sons, New York, 1998.

[5] J. Hong, J. C. Akers, R. Venugopal, M. N. Lee, A. G. Sparks, P. D. Washabaugh and D. S. Bernstein, "Modeling, Identification and Feedback Control of Noise in an Acoustic Duct," *IEEE Transactions on Control Systems Technology*, Vol. 41, pp. 283-291, May 1996.

[6] R. S. Erwin and D. S. Bernstein, "Fixed-Structure Discrete-Time Mixed H_2/H_∞ Controller Synthesis Using the Delta-Operator," *Proc. Amer. Contr. Conf.*, pp. 3526-3530, Albuquerque, NM, June 1997.

[7] R. S. Erwin and D. S. Bernstein, "Discrete-Time H_2/H_∞ Control of an Acoustic Duct: δ-domain Design and Experimental Results," *Proc. IEEE Conf. Dec. Contr.*, pp. 281-282, San Diego, CA, December 1997.

[8] S. M. Kuo and D. R. Morgan, *Active Noise Control Systems*, Wiley, New York, 1996.

[9] P. A. Nelson and S. J. Elliot, *Active Control of Sound.* New York: Academic Press, 1992.

[10] D. G. MacMartin, "A Feedback Perspective on the LMS Disturbance Feedforward Algorithm," *Proceedings of the American Control Conference*, Baltimore, MD, pp. 1632 - 1636, 1994.

[11] T. Van Pelt, R. Venugopal, and D. S. Bernstein, "Experimental Comparison of Adaptive Cancellation Algorithms for Active Noise Control," *Proc. Conf. Contr. Appl.*, Hartford, CT, pp. 559-564, October 1997.

[12] R. Venugopal and D. S. Bernstein, "Adaptive Disturbance Rejection using ARMARKOV System Representations," *IEEE Trans. Contr. Sys. Tech.*, Vol. 8, pp. 257-269, March 2000.

[13] H. Sane, R. Venugopal, and D. S. Bernstein, "Disturbance Rejection Using Self-Tuning ARMARKOV Adaptive Control with Simultaneous Identification," *Proc. Amer. Contr. Conf.*, pp. 2040-2044, San Diego, CA, June 1999; *IEEE Trans. Contr. Sys. Tech*, to appear.

[14] H. Sane and D. S. Bernstein, "Active Noise Control Using an Acoustic Servovalve," *Proc. Amer. Contr. Conf.*, pp. 2621-2625, Philadelphia, PA, June 1998.

[15] S. J. Elliot, I. M. Stothers and P. A. Nelson, "A Multiple Error LMS Algorithm and its Applications to the Active Control of Sound and Vibration," *IEEE Trans. Acoustics, Speech, Signal Processing*, Vol. ASSP-35, pp. 1423-1434, 1987.

[16] J. Hong and D. S. Bernstein, "Bode Integral Constraints, Colocation, and Spillover in Active Noise and Vibration Control," *IEEE Trans. Contr. Sys. Tech.*, Vol. 6, pp. 111-120, 1998.

[17] S. L. Lacy, R. Venugopal, and D. S. Bernstein, "ARMARKOV Adaptive Control of Self-Excited Oscillations of a Ducted Flame," *Proc. Conf. Dec. Contr.*, pp. 4527-4528, Tampa, FL, December 1998.

[18] R. Venugopal, H. S. Sane, D. P. Scharf, D. S. Bernstein and D. C. Hyland, "Disturbance Rejection Using Decentralized Self-Tuning ARMARKOV Adaptive Control with Simultaneous Identification ," *Proc. Amer. Inst. Aero. Astro. Conf. Guid., Nav. Contr.*, Denver, CO, Aug. 2000.

[19] J. C. Akers and D. S. Bernstein, "Time-Domain Identification Using ARMARKOV/Toeplitz Models," *Proc. Amer. Contr. Conf.*, Albuquerque, NM, pp. 191-195, June 1997.

[20] P. Van Overschee and B. De Moor, "N4SID: Subspace algorithms for identification of combined deterministic-stochastic systems," *Automatica*, Vol. 30, pp. 75-93, Jan. 1994.